Thermal Maturation of Gas Shale Systems

Sylvain Bernard[1] and Brian Horsfield[2]

[1]Institut de Minéralogie, de Physique des Matériaux et de Cosmochimie, Centre National de la Recherche Scientifique, UMR 7590, Sorbonne Universités, Muséum National d'Histoire Naturelle, Université Pierre et Marie Curie (Paris 6), IRD 206, 75005 Paris, France; email: sbernard@mnhn.fr

[2]GFZ German Research Centre for Geosciences, 14473 Potsdam, Germany; email: brian.horsfield@gfz-potsdam.de

Annu. Rev. Earth Planet. Sci. 2014. 42:635–51

The *Annual Review of Earth and Planetary Sciences* is online at earth.annualreviews.org

This article's doi: 10.1146/annurev-earth-060313-054850

Keywords

unconventional gas, shale diagenesis, late gas, microstructure, porosity, pyrobitumen

Abstract

Shale gas systems serve as sources, reservoirs, and seals for unconventional natural gas accumulations. These reservoirs bring numerous challenges to geologists and petroleum engineers in reservoir characterization, most notably because of their heterogeneous character due to depositional and diagenetic processes but also because of their constituent rocks' fine-grained nature and small pore size—much smaller than in conventional sandstone and carbonate reservoirs. Significant advances have recently been achieved in unraveling the gaseous hydrocarbon generation and retention processes that occur within these complex systems. In addition, cutting-edge characterization technologies have allowed precise documentation of the spatial variability in chemistry and structure of thermally mature organic-rich shales at the submicrometer scale, revealing the presence of geochemical heterogeneities within overmature gas shale samples and, notably, the presence of nanoporous pyrobitumen. Such research advances will undoubtedly lead to improved performance, producibility, and modeling of such strategic resources at the reservoir scale.

1. INTRODUCTION

Gas shales are geological formations of economic significance as they constitute an established target for commercial hydrocarbon production. Owing to its abundance, shale gas has increasingly attracted worldwide attention (**Figure 1**) (Armor 2013, McGlade et al. 2013, Weijermars 2013, Xingang et al. 2013), and with more than 100 years' worth of worldwide reserves as estimated by the US Energy Information Administration (EIA; **http://www.eia.gov**), it holds promise as a sustainable energy source for the foreseeable future. In the United States, following the establishment in the 2000s of commercial gas production from the Barnett Shale (Texas), successful exploration rapidly expanded to other shale gas plays, notably the Fayetteville Shale (Arkansas), the Woodford Shale (Oklahoma), the Haynesville Shale (Louisiana and Texas), and the Marcellus Shale (Pennsylvania). As a result, shale gas rose from less than 1% to more than 20% of US domestic gas production between 2000 and 2010, and according to EIA projections it will likely account for more than 45% of the US gas supply by 2035 (**Figure 1**).

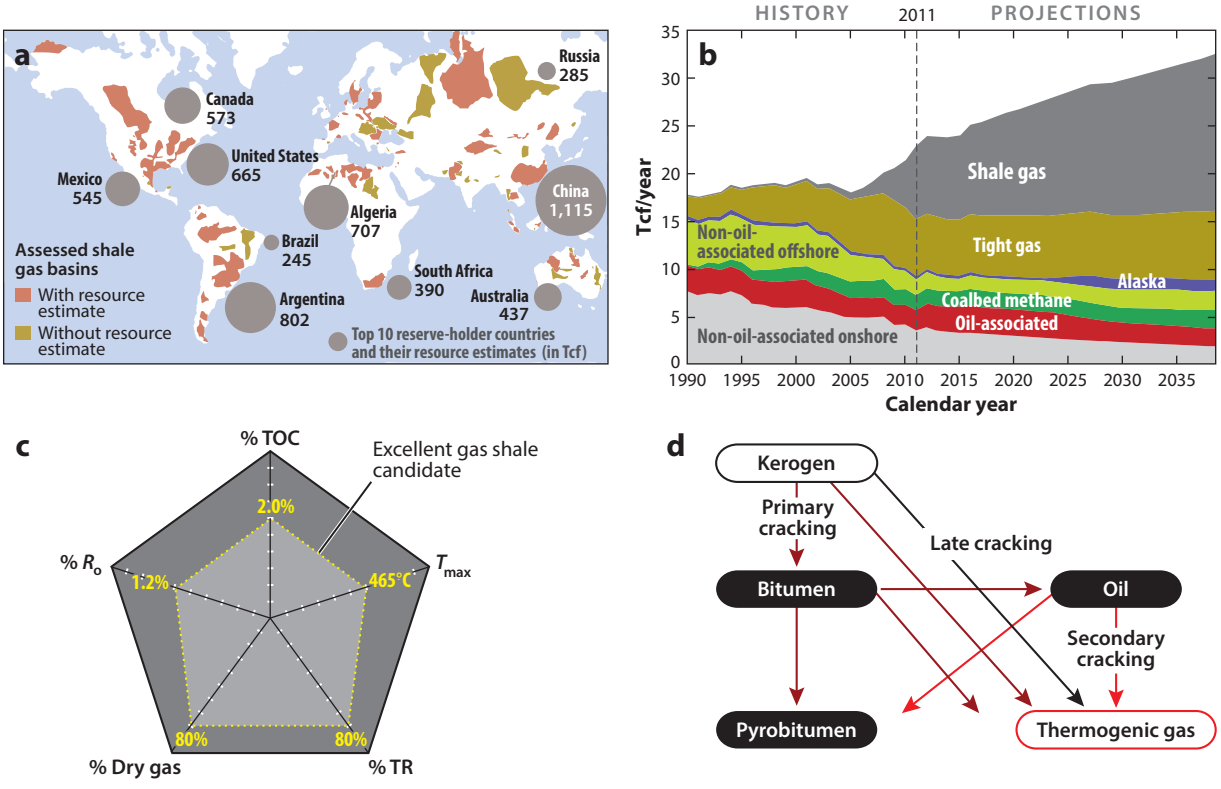

Figure 1

(*a*) Map of the world's largest shale gas deposits (from US EIA 2013). (*b*) US natural gas production by source for the period 1990–2040 (from US EIA 2013). (*c*) Polar shale gas risk plot (Hill plot) showing the minimum values of total organic content (wt% TOC), maturity level (% R_o and T_{max}), gas dryness (% dry gas), and transformation ratio (% TR) required for a gas shale formation to ensure gas production (modified from Jarvie et al. 2007). (*d*) Sketch illustrating source rock processes in gas shales that lead to thermogenic gas generation (modified from Jarvie et al. 2007). Abbreviation: Tcf, trillion cubic feet.

Unlike conventional systems, gas shales constitute self-contained source-reservoir systems of large, continuous (unconventional) dimensions. They are characterized by widespread gas saturation, subtle trapping mechanisms, seals of variable lithology, and relatively short hydrocarbon migration distances (e.g., Curtis 2002, Jarvie et al. 2007, Boyer et al. 2011). Understanding the geological and geochemical nature of gas shale formation and improving gas recovery have recently been at the heart of millions of dollars' worth of research. Almost all currently producing shale gas reservoirs are organic-rich overmature oil source rocks in the thermogenic gas window that are sufficiently brittle and rigid to allow hydraulic fracturing for production in commercial quantities (e.g., Curtis 2002, Jenkins & Boyer 2008, Boyer et al. 2011). Production performance and recovery from unconventional reservoirs are highly variable between basins and within individual plays. Due to the interdependence of geology, geochemistry, geomechanics, and petrophysics on productivity and recovery, an integrated understanding of geologic controls (such as mineralogy, rock textures, depositional environment, and present-day and paleostresses) is required for interpreting production behavior and predicting future success.

Artificial maturation and pyrolysis experiments performed in the laboratory under well-constrained physical and chemical conditions have been extensively used for decades to better constrain the hydrocarbon generation processes occurring in source rocks (Lewan et al. 1979; Horsfield & Dueppenbecker 1991; Horsfield et al. 1992; Schenk et al. 1997; Stasiuk 1997; Seewald et al. 1998; Hill et al. 2003; Behar et al. 2008, 2010; Tiem et al. 2008; Lewan & Roy 2011; Pan et al. 2012). The main issue with these experiments is that temperatures and heating rates considerably higher than those encountered in nature must be applied to the rock samples to simulate long geological time periods. Although extrapolating laboratory results to natural hydrocarbon generation processes covers nine orders of magnitude, and thereby may be deemed perilous (e.g., Snowdon 1979), predictions have proven to be robust where correlations are available (e.g., Schenk & Dieckmann 2004, Kuhn et al. 2012).

Full well-log suites, including high-resolution density and resistivity logs and borehole images, can be used to derive porosity, fluid saturation, and permeability estimations. In addition, a wide range of bulk analyses are now routinely used to estimate the content and type of kerogen and bitumen present, the level of maturity, and the amount and type of hydrocarbons potentially generated within gas shale formations worldwide (e.g., Horsfield 1989, Curtis 2002, Jenkins & Boyer 2008, Boyer et al. 2011). In parallel, nondestructive spectroscopic analyses, such as solid-state nuclear magnetic resonance, Fourier transform infrared spectroscopy, and X-ray absorption near edge structure (XANES) spectroscopy, are increasingly used to chemically and structurally characterize natural kerogen and its degradation products (e.g., Lis et al. 2005; Wei et al. 2005; Smernik et al. 2006; Kelemen et al. 2007; Petersen et al. 2008; Mao et al. 2010; Bernard et al. 2012a,b).

Not surprisingly, given that the fundamental microstructural and geochemical properties of gas shales differ markedly from those of traditional petroleum reservoirs, the application and interpretation of many conventional analysis techniques have proven to be more complex for such unconventional source-reservoir systems (Loucks et al. 2009, Wang & Reed 2009, Ambrose et al. 2010, Curtis et al. 2010, Dacy 2010, Sondergeld et al. 2010, Elgmati et al. 2011a, Chalmers et al. 2012a, Josh et al. 2012, Bai et al. 2013). As a result, traditional continuum models describing flow in porous media that are widely applicable in conventional gas reservoirs are not applicable in unconventional gas-rich systems, in which flow appears to be controlled by diffusion (Javadpour et al. 2007, Bustin et al. 2008, Bustin & Bustin 2012, Chalmers et al. 2012b). Thus, as detailed in this article, recent efforts have focused on better assessing the geochemical nature of the various constituents of gas shale systems as well as on better documenting their microstructure down to the nanometer scale.

2. GASEOUS HYDROCARBON GENERATION PROCESSES

Shales display compositions that vary laterally and vertically due to the effects of depositional and diagenetic processes. Ideal gas shales are mudrocks that were deposited under anoxic conditions and—as for the Barnett Shale, for example—in an oxygen minimum zone developed beneath highly productive upwelling waters (e.g., Jarvie et al. 2007, Slatt & Rodriguez 2012). So-called Type II organic matter formed in such environments from mainly planktonic debris has a very high generation capacity, with up to 750 mg hydrocarbon for each gram of organic carbon.

Key parameters used in evaluating shale resources address the degree to which this full potential can be realized and in what form, and include total organic content (wt% TOC), thermal maturity level (% R_o and T_{max}), transformation ratio (% TR), and gas dryness (% dry gas) (**Figure 1**) (e.g., Jarvie et al. 2007, Dembicki 2009). Increasing gas dryness accompanies progressive maturation. The gas shale content of nonhydrocarbon gases such as CO_2 and H_2S is usually low (e.g., Armor 2013).

Four distinct processes may result in the formation of thermogenic gaseous hydrocarbons (**Figure 1**) (Lewan et al. 1979, Pepper & Corvi 1995, Pepper & Dodd 1995, Schenk et al. 1997, Lorant & Behar 2002, Erdmann & Horsfield 2006, Jarvie et al. 2007, Tian et al. 2008, Guo et al. 2009): (*a*) the decomposition of kerogen to gas and bitumen, (*b*) the secondary decomposition of bitumen to oil and gas, (*c*) the secondary cracking of oil to gas and a carbon-rich residue such as pyrobitumen, and (*d*) the degradation of overmature kerogen within the metagenesis zone, leading to the formation of late gas. The relative importance of each depends upon the temperature-time conditions that together bring about thermal cracking reactions. Primary kerogen cracking occurs between temperatures of 80°C and 180°C for 10% and 90% conversion, respectively, whereas secondary oil-to-gas cracking has been suggested to begin at approximately 150°C, depending on heating rate (e.g., Dieckmann et al. 1998). Notably, some bitumen components consisting primarily of asphaltenes and resins crack at the same time as or soon after their formation from kerogen (Behar et al. 2010).

Most of the crude oil and gas generated in organic-rich shales are expelled into adjacent carrier systems (Cooles et al. 1986). Yet, due to very low permeabilities, generated oil and gas fail to fully escape their original shale source rock because they lack a viable migration path (Nelson 2009). Generated gas can be stored in porosity and fractures, adsorbed onto kerogen and clay particles, or dissolved in kerogen and (pyro)bitumen (e.g., Curtis 2002, Montgomery et al. 2005, Jarvie et al. 2007, Loucks et al. 2009, Ross & Bustin 2009, Strapoc et al. 2010). The mass of gas in place within a gas shale is equal to the mass of labile organic matter times the degree of conversion times the retention efficiency times the proportion of gaseous products times the percent hydrocarbons in that gas. High conversion levels allow intrinsic potential to be realized. The sweet spot for gas occurrence in the Barnett, Fayetteville, and Woodford Shales occurs at high conversion of about 90%, above a vitrinite reflectance level of approximately 1.1–1.3% (e.g., Jarvie et al. 2007). This value of R_o corresponds to the onset of secondary gas generation from primary liquids (C_{6+} organics) predicted using kinetic modeling (Dieckmann et al. 1998). Secondary cracking in shales thus occurs at a maturity level significantly lower than that predicted for the onset of oil-to-gas cracking (approximately 2% R_o) in conventional siliciclastic reservoirs, possibly pointing to autocatalytic activity (Horsfield et al. 1992, Schenk & Horsfield 1998).

Thanks to the dramatic increase in shale penetrations brought about by shale gas exploration, new insights are being gained into how they evolve at high levels of maturity (Rodriguez & Philp 2010, Tilley et al. 2011, Zumberge et al. 2012, Hao & Zou 2013). Included here is the rollover of ethane and propane $\delta^{13}C$ values ($\delta^{13}C_2$ and $\delta^{13}C_3$ initially increase and then decrease as thermal maturity increases) and isotopic reversals among methane, ethane, and propane (e.g., Hao &

Zou 2013). Such isotopic distribution patterns from normal through partial reversal to complete reversal have been proposed to result from the simultaneous cracking of kerogen, retained oil, and wet gas in closed systems, i.e., where low oil expulsion efficiency at peak oil generation, low expulsion efficiency at peak gas generation, and little gas loss during postgeneration evolution have occurred (Hao & Zou 2013).

The disproportionation of hydrogen that occurs during secondary cracking results in the formation of hydrogen-rich species (e.g., dry and wet gases) and hydrogen-poor species (pyrobitumen) and is accompanied by shrinkage to form secondary porosity (see below for detailed discussion). Maximum secondary gas yield is controlled by the yield of C_{6+} precursors available for secondary cracking, which in turn is determined by the efficiency of petroleum expulsion at lower (oil window) maturity levels (Mahlstedt & Horsfield 2012). According to the algebraic mass balance model of Cooles et al. (1986), organic-rich shales are excellent expellers of petroleum (approximately 90%), meaning that masses of retained gas are accordingly low; Jarvie et al. (2007) are more conservative in their assessment of expulsion (65%), pointing to higher in-place gas yield estimates. Intriguingly, shales with lower organic richness are poor expellers (i.e., good retainers); as such, they are unable to source conventional petroleum but are potentially good gas shales. As the volume of gas generated within gas shales by secondary cracking directly depends on oil retention in the system, it thus depends on the nature of organic and inorganic phases and their specific adsorption capabilities as well as on organic-inorganic structural relationships, pores, and fracture networks. Chemical and physical changes that occur within gas shales during thermal maturation are intricately interdependent.

The sorption capacities of gas shales may drastically vary during burial and subsequent uplift. This variability is mainly due to variations in pressure and temperature conditions, although the microstructure of organic matter, which directly results from its type and maturity level, may also control the capacity of the surfaces (Muscio et al. 1994, Krooss et al. 2002, Mahlstedt et al. 2008). Oversaturation and gas leak-off may occur during uplift (e.g., Littke et al. 2011). At that time, if oil or condensate is also present, phase changes occur, leading to the development of two-phase systems that comprise a gas-rich phase associated with a second phase enriched in heavier hydrocarbons (di Primio et al. 1998, di Primio 2002). Thus, although the timing of oil and gas generation from kerogen throughout the oil window is critical for trap formation in conventional petroleum systems, it is not that essential for shale gas systems. Even though in the case of marine source rocks primary gas-oil ratios are low overall throughout the oil window, secondary cracking and physical fractionation can lead to enrichment in gas (e.g., Santamaria-Orozco & Horsfield 2003). Indeed, mature kerogen and pyrobitumen build a late gas potential with increasing maturation. It was initially thought that recombination processes could explain significant dry gas potential at very high maturity levels (approximately 2% R_o) and high geological temperatures (>200°C) (Dieckmann et al. 2006, Erdmann & Horsfield 2006) and that mainly terrigenous organic matter evolved in this way. Yet, high late gas potentials are associated with all organic matter types, and directly associated with the alpha cleavage of residual methyl groups (**Figure 2**) (Mahlstedt et al. 2008, Mahlstedt & Horsfield 2012).

3. METHODOLOGICAL ISSUES FOR THE MICROSTRUCTURAL CHARACTERIZATION OF GAS SHALES

Shale gas reservoirs possess a high degree of complexity, demonstrating heterogeneity from the reservoir scale down to the nanoscale. Such complexity has been recognized since the earliest petrographic examinations of shales (Sorby 1908). Gas shale systems do not form homogeneous and featureless deposits but instead exhibit chemical and mineralogical heterogeneities at the

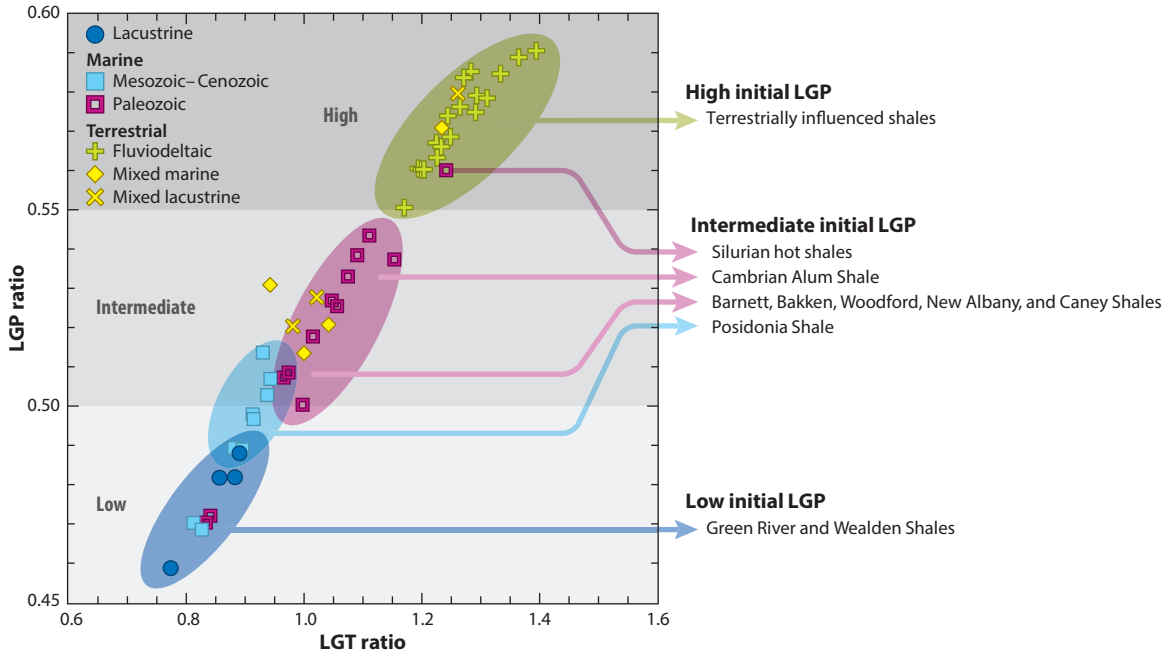

Figure 2

Late gas potential (LGP) ratio and late gas type (LGT) ratio of various gas shale systems based on the analysis of immature samples. These ratios have been determined on the basis of high-temperature, nonisothermal, closed-system microscale sealed-vessel (MSSV) pyrolysis gas chromatography experiments (Mahlstedt & Horsfield 2012). The LGP ratio is defined as the ratio of the gas yield at 700°C to the sum of gas yields at 560°C and 700°C. Source rocks generating late gas exhibit an LGP ratio greater than 0.5. The LGT is defined as the ratio of the gas yield at 700°C to the sum of gas yield at 560°C and the yield of late gas derived from cracking of C_{6+} compounds. LGT ratios less than 1 are seen for source rocks whose late gas potential is due mainly to C_{6+} cracking, whereas LGT ratios greater than 1 are seen for source rocks whose late gas potential can be explained only by a thermally stable, refractory moiety, which yields additional amounts of secondary late gas at late temperature stages. Modified from Mahlstedt & Horsfield (2012).

submicrometer scale, as a direct result of their depositional environments and postdepositional diagenetic processes (e.g., Arthur & Sageman 1994, Katsube & Williamson 1994, Ross & Bustin 2009, Loucks et al. 2009, Bernard et al. 2010b). Macroscopic averaging methods such as low-pressure adsorption isotherms (e.g., Bustin et al. 2008), high-pressure mercury intrusion porosimetry (e.g., Nelson 2009), solid-state nuclear magnetic resonance (e.g., Sondergeld et al. 2010), and small-angle and ultra-small-angle neutron scattering (e.g., Clarkson et al. 2012, 2013; Ruppert et al. 2013) have shown that pore sizes within gas shales are on the order of a few nanometers to tens of nanometers. At this scale, conventional continuum descriptions of gas transport do not apply. Owing to this nanoscale porosity, which is orders of magnitude smaller than that in conventional reservoirs (**Figure 3**), flow equations and mathematical models originally developed for conventional sandstone and carbonate hydrocarbon reservoirs are not directly applicable to shales. Type, size, and arrangement of pores at the nanoscale may strongly affect hydrocarbon storage and sealing capacity (e.g., Ambrose et al. 2010, Schieber 2010). In addition, differences in the origin and distribution of pore types may affect permeability and wettability (e.g., Nelson 2009, Passey et al. 2010).

The need to better document the pore structure of gas shale systems has recently become a challenge for organic geochemical research (Loucks et al. 2009, 2010, 2012; Curtis et al. 2010, 2011a,b, 2012a–c; Passey et al. 2010; Schieber 2010; Heath et al. 2011; Slatt & O'Brien 2011;

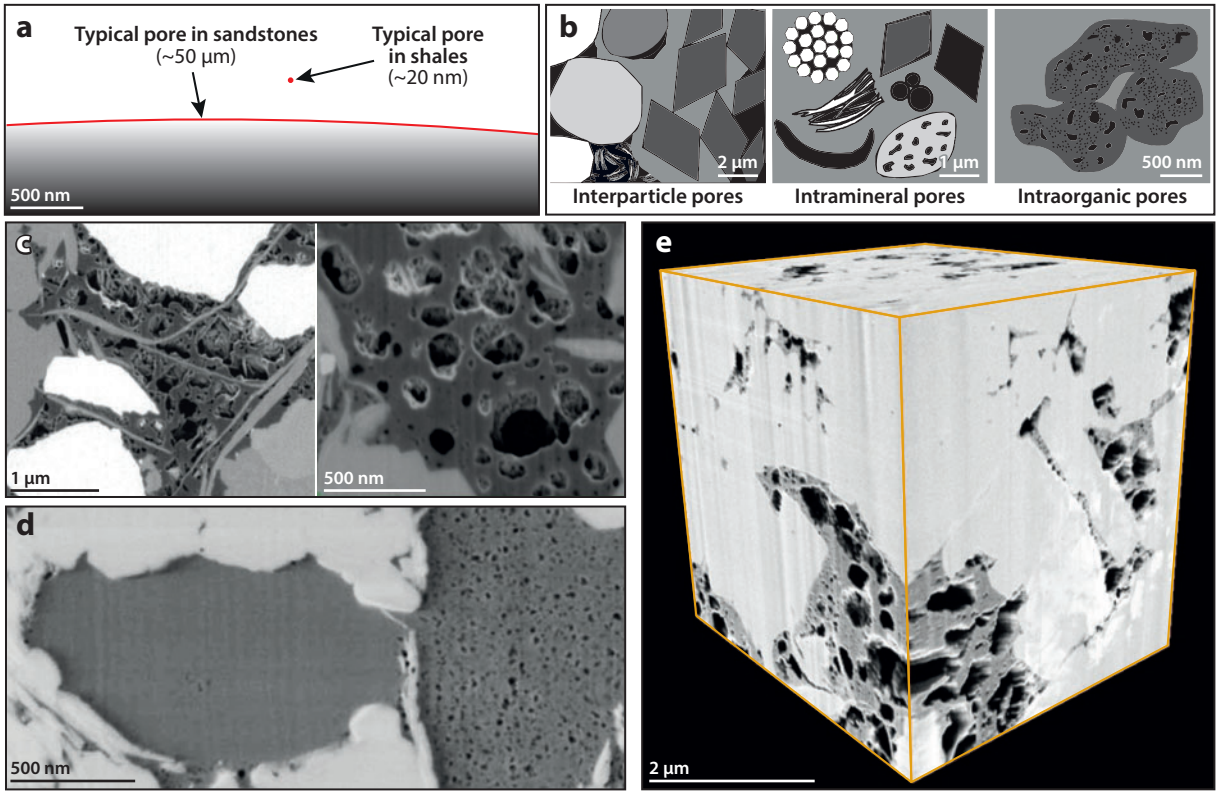

Figure 3

(*a*) Difference in typical pore sizes between sandstones and shales. (*b*) Different types of pores (*black*) following the classification of Loucks et al. (2010, 2012): interparticle, intramineral, and intraorganic (modified from Loucks et al. 2012). (*c*) Focused ion beam scanning electron microscopy (FIB-SEM) images in backscattered electron (BSE) mode of an overmature Horn River Shale sample. Organic matter appears dark and displays irregularly shaped, roughly circular nanopores; mineral grains are visible in various lighter shades of gray and pyrite in white (modified from Curtis et al. 2010). (*d*) FIB-SEM image in BSE mode of an overmature Woodford Shale sample, showing the coexistence of nonporous and nanoporous organic masses (*dark regions*) (modified from Curtis et al. 2012b). (*e*) Three-dimensional FIB-SEM volume in BSE mode of an overmature Eagle Ford Shale sample, showing nanoporous organic masses (*dark regions*) (modified from Walls & Sinclair 2011).

Walls & Sinclair 2011; Bernard et al. 2012a,b; Driskill et al. 2013). Imaging gas shale nanopores requires high-quality preparation and imaging techniques that allow fine details of microstructure to be preserved with minimal artifacts. Confocal laser scanning microscopy and conventional scanning electron microscopy (SEM) are inadequate to characterize submicrometer grains and pores from broken or mechanically polished shale samples. Argon ion beam milling has thus increasingly been used to overcome this difficulty by producing ultrasmooth polished surfaces that allow high-magnification SEM to be performed at high spatial resolution (Loucks et al. 2009; Wang & Reed 2009; Desbois et al. 2010, 2013; Curtis et al. 2011a,b). Atomic force microscopy has also been successfully used to characterize mudrock nanopores (Javadpour 2009, Javadpour et al. 2012). Recent advancements in focused ion beam scanning electron microscopy (FIB-SEM) systems have offered another alternative for investigating the three-dimensional submicrometric fabric of a variety of samples (Curtis et al. 2010, 2011a,b, 2012a; Desbois et al. 2010; Sondergeld et al. 2010; Bera et al. 2011; Elgmati et al. 2011a,b; Heath et al. 2011; Walls & Sinclair 2011;

Chalmers et al. 2012a; Bernard et al. 2013; Driskill et al. 2013). The FIB-SEM technique can also be used to extract ultrathin (<100-nm-thick) sections of sample across areas of interest, thus providing suitable samples for transmission electron microscopy, which offers a unique combination of chemical and structural information with unsurpassed spatial resolution (Bernard et al. 2010a,b; Curtis et al. 2011b; Chalmers et al. 2012a). These recent studies have reported a variety of pore types in thermally mature gas shales. Although various porosity classification schemes exist (Orr 1977, Kwon et al. 2004, Desbois et al. 2010, Milliken & Reed 2010, Heath et al. 2011), the descriptive approach introduced by Loucks et al. (2010, 2012), which groups shale matrix-related pores into three basic categories on the basis of their relationships to organic and inorganic particles, is perceived as the most convenient to use and the most consistent with schemes of pore subdivisions that have been used for decades in conventional carbonate and sandstone reservoir systems (e.g., Choquett & Pray 1970, Pittman 1979). In this scheme, pore types include interparticle pores, intramineral pores, and intra-organic-matter (intraorganic) pores (**Figure 3**). Most of the recent studies have documented intraorganic pores that have irregular, bubble-like, elliptical cross sections and generally range between 5 and 500 nm in length in thermally mature gas shales (**Figure 3**) (Loucks et al. 2009, 2010, 2012; Passey et al. 2010; Elgmati et al. 2011a,b; Heath et al. 2011; Slatt & O'Brien 2011; Walls & Sinclair 2011; Bernard et al. 2012a,b; Curtis et al. 2012a–c).

4. DIAGENETIC EVOLUTION OF SHALE PORES ASSOCIATED WITH THE MINERAL MATRIX

The burial diagenesis and transformation of organic-rich muds to highly heterogeneous organic-rich shales form a complex process that is a function of many variables, including original mineralogy, fabric, texture, organic content, fluids, hydrology, and burial rate and depth. Diagenesis may significantly affect shale porosity and permeability (Katsube & Williamson 1994, Kim et al. 1999, Ross & Bustin 2009, Yang & Aplin 2010, Schneider et al. 2011, Emmanuel & Day-Stirrat 2012, Milliken et al. 2012), which can range over more than an order of magnitude (e.g., Mondol et al. 2008, Mehmani et al. 2011). The pores associated with the mineral matrix include interparticle pores and intramineral pores (Loucks et al. 2010, 2012). Interparticle pores have varying origins, and their geometries differ significantly as a function of both primary pore preservation and diagenetic alteration (Loucks et al. 2012). Indeed, interparticle pores are highly sensitive to burial-induced mechanical compaction (Aplin et al. 2006, Loucks et al. 2012, Bernard et al. 2013). In immature sediments, the typically abundant and well-connected interparticle pores may form an effective (permeable) pore network (Klaver et al. 2012). However, with increasing burial and overburden stress, compaction and cementation processes make this early-formed interparticle porosity collapse (Kim et al. 1999, Mondol et al. 2008, Milliken & Reed 2010, Mehmani et al. 2011). Given that shales experience the fastest rates of compaction during the first kilometer of burial, the main phase of interparticle pore collapse likely occurs before the initiation of any significant volume of hydrocarbon generation (Loucks et al. 2012, Bernard et al. 2013).

In contrast to interparticle pores, as defined by Loucks et al. (2010, 2012), intramineral pores occur within mineral boundaries and can be primary (i.e., original pores within grains that are clustered together, such as intercrystalline pores within pyrite framboids) or secondary (e.g., dissolution pores, such as intracrystalline pores within calcareous fossils) in origin. Thus, by definition, intramineral pores are less likely than are interparticle pores to be part of an effective pore network, because they are likely less interconnected. Although intramineral pores are less sensitive to mechanical diagenesis (compaction), their number and volume appear to be strongly controlled by chemical diagenesis, i.e., by authigenesis and dissolution/precipitation processes (Loucks et al. 2012, Bernard et al. 2013). Although diagenetic cementation processes can completely occlude

the intramineral pore spaces, secondary intramineral pores may locally form, most likely as the result of organic matter thermal decarboxylation (e.g., Mazzullo & Harris 1992, Ehrenberg et al. 2012). Notably, in thermally mature gas shales, most of the intramineral pore spaces are filled with bitumen, indicating that they were once sufficiently interconnected to allow bitumen to migrate (Loucks et al. 2012, Bernard et al. 2013).

5. ORIGIN AND NATURE OF NANOPOROUS ORGANIC PARTICLES

Since the pioneer study performed by Loucks et al. (2009), the discovery of organic compounds exhibiting irregular-ellipsoid-shaped nanopores of approximately 5 to 500 nm has been reported in most gas shale systems worldwide (**Figures 3** and **4**), including the Barnett Shale (Curtis et al. 2010, 2011b, 2012a; Loucks et al. 2010, 2012; Passey et al. 2010; Slatt & O'Brien 2011; Bernard et al. 2012b), the Marcellus Shale (Curtis et al. 2011b, 2012a), the Woodford Shale (Curtis et al. 2011a,b, 2012a–c), the Horn River Shale (Curtis et al. 2011b, 2012a), the Eagle Ford Shale (Walls & Sinclair 2011, Curtis et al. 2012a), the Gothic Shale (Heath et al. 2011), the Haynesville Shale (Curtis et al. 2011b), the Utica Shale (Elgmati et al. 2011a), the Tuscaloosa Shale (Heath et al. 2011), the Fayetteville Shale (Elgmati et al. 2011b, Bai et al. 2013) and the Posidonia Shale (Bernard et al. 2012a, 2013). This nanoporosity may constitute as much as 50% of the volume of a single organic particle (Curtis et al. 2010, 2012a; Loucks et al. 2010, 2012). In agreement with the prediction of Loucks et al. (2009), Ambrose et al. (2010) and Sondergeld et al. (2010) have recently provided evidence that these intraorganic pores may form a connected three-dimensional effective pore network through the interconnectivity of organic particles. Thus, although intraorganic nanopores do not necessarily dominate in total volumetric contribution, the three-dimensional arrangement of nanoporous organic particles likely has a substantial influence on the gas storage capacity and permeability of thermally mature gas shales (e.g., Ambrose et al. 2010, Passey et al. 2010, Sondergeld et al. 2010, Slatt & O'Brien 2011, Curtis et al. 2012a, Loucks et al. 2012).

As demonstrated by detailed studies of maturation series, there is no doubt that this particular pore type is acquired during increasing thermal maturation (**Figure 4**) (Bernard et al. 2012a,b; Curtis et al. 2012b,c; Loucks et al. 2012). Despite their ubiquity, however, the chemical nature of these nanoporous organic compounds has long remained puzzling. The differential evolution of various organic matter types has been proposed to explain the co-occurrence of nonporous and nanoporous organics in overmature gas shales (Curtis et al. 2012a,b). Variable volume changes during late conversion of kerogen to hydrocarbons have been suggested to induce the creation of such porosity, even within the oil window (e.g., Loucks et al. 2009, 2012). Yet, the use of synchrotron-based scanning transmission X-ray microscopy (STXM), which allows XANES spectroscopy to be performed at high spatial resolution, thus providing information on organic constituent speciation at the 20-nm scale (e.g., Kilcoyne et al. 2003, Bluhm et al. 2006, Kaznatcheev et al. 2007, Bernard et al. 2009), has recently led to the interpretation that this nanoporosity results from the exsolution of gaseous hydrocarbons during the secondary thermal cracking of retained oil (e.g., Bernard et al. 2012a,b). The XANES signatures of nanoporous organic particles from thermally mature samples of Barnett and Posidonia Shales are indeed consistent with thermally altered bitumen—i.e., as pyrobitumen compounds—while the nonporous organic particles observed within the same samples exhibit XANES signatures consistent with overmature kerogen (**Figure 4**) (Bernard et al. 2012a,b). Surprisingly, the XANES signatures of bitumen and nanoporous pyrobitumen residues in the samples investigated in these studies reveal a significant concentration of heteroatoms, which have been interpreted as partly resulting from hydrothermal brine circulation (Bernard et al. 2012a,b).

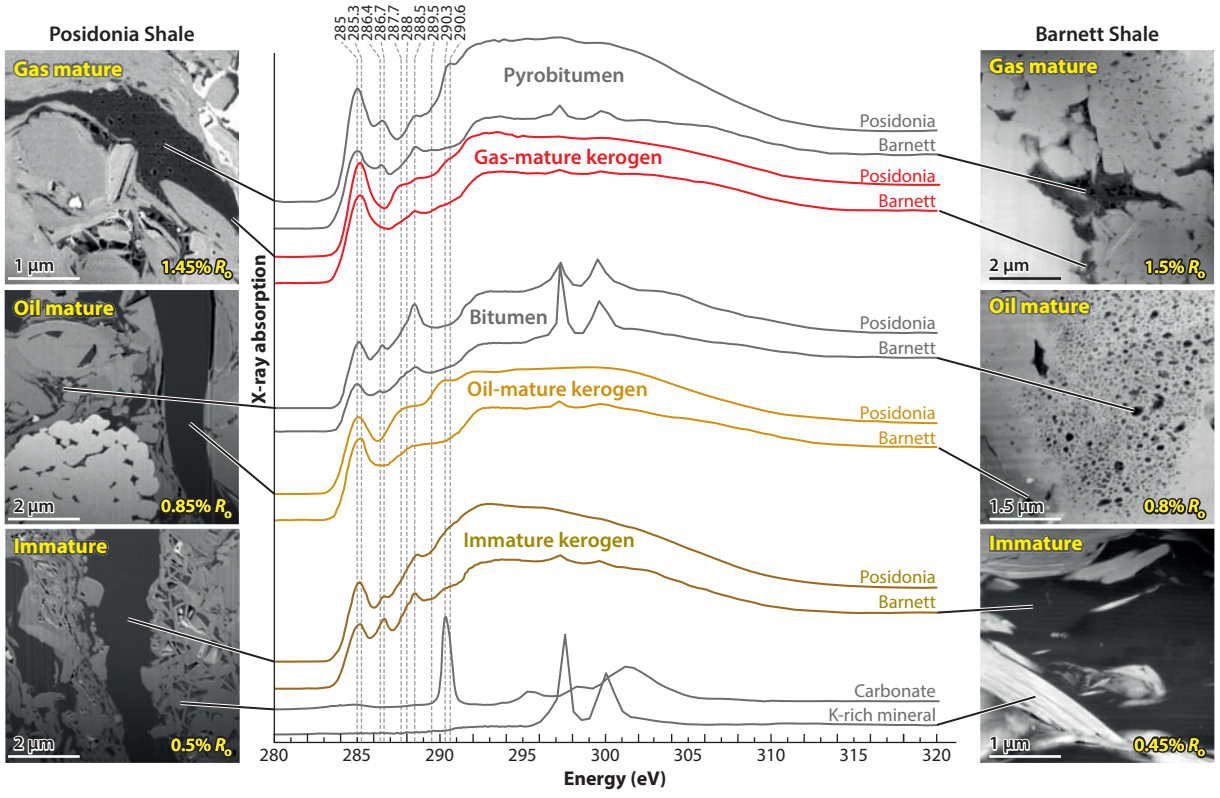

Figure 4

Focused ion beam scanning electron microscopy (FIB-SEM) images in backscattered electron (BSE) mode of three Posidonia Shale samples (*left*) and scanning transmission electron microscopy (STEM) images in high-angle annular dark-field (HAADF) mode of three Barnett Shale samples (*right*), showing organic matter (*dark regions*). These two sets of samples constitute two natural maturation series. Organic masses evolve from nonporous immature kerogen in immature samples ($R_o \approx 0.5\%$) to bitumen and nonporous oil-mature kerogen in oil-mature samples ($R_o \approx 0.8\%$) and to nonporous gas-mature kerogen and nanoporous pyrobitumen in gas-mature samples ($R_o \approx 1.5\%$). The scanning transmission X-ray microscopy (STXM)-based X-ray absorption near edge structure (XANES) spectra of these different organic compounds are shown in the center. Absorption features at 285 and 285.3 eV are attributed to electronic transitions of aromatic groups; 286.4 and 286.7 eV to ketonic or phenolic groups; 287.7 and 288 eV to aliphatic groups; 288.5 eV to hydroxyl groups; 289.5 eV to carbonate groups; and 290.3 and 290.6 eV to alkyl carbon. Modified from Bernard et al. (2012a,b, 2013).

6. CONCLUDING REMARKS

In contrast to conventional systems, gas shales constitute self-contained source-reservoir systems of large continuous (unconventional) dimensions. Because the fundamental microstructural and geochemical properties of gas shales differ markedly from those of traditional petroleum reservoirs, many conventional analysis techniques have proven more complex to apply and interpret for such unconventional source-reservoir systems. As detailed in this article, recent efforts have been made to better assess the geochemical nature of the various constituents of gas shale systems and to better document their microstructure down to the nanoscale. Although key scientific questions regarding transport mechanisms in unconventional gas shale reservoirs remain, these recent efforts will undoubtedly help to improve the reliability of the kinetic models used to predict the amount and composition of hydrocarbons generated within such complex self-contained source-reservoir systems. Because of the high degree of interdependence between rock fabric,

gas transport, and recovery in such unconventional reservoirs, forthcoming research should focus on better understanding the fundamental physics governing transport in order to facilitate exploration and production efforts.

SUMMARY POINTS

1. Shale gas systems do not form homogeneous and featureless deposits but instead exhibit microscale and nanoscale chemical and mineralogical heterogeneities, which directly result from their depositional environments and diagenetic processes.
2. Thermal cracking of organic matter with a high generation potential, followed by secondary cracking of liquids, and lastly by cracking of residual methyl groups, forms the major portion of the gas.
3. The changes in temperature and especially pressure during uplift cause migration and fractionation effects associated with changes in adsorptive properties and gas-liquid phase behavior, respectively.
4. Imaging gas shale nanopores requires high-quality preparation and imaging techniques such as argon milling or FIB-SEM imaging to preserve the fine details of microstructure with minimal artifacts.
5. In addition to pores related to the mineral matrix, most of the recent studies have documented intraorganic pores that have irregular, bubble-like, elliptical cross sections and generally range between 5 and 500 nm in length in thermally mature gas shales.
6. The use of synchrotron-based STXM has recently allowed the nanoporous organic particles observed within thermally mature gas shale samples to be identified as thermally altered bitumen, i.e., as pyrobitumen compounds.

FUTURE ISSUES

1. Key scientific questions remain regarding the fundamental physics governing transport mechanisms within and mechanical properties of unconventional gas shale reservoirs to ensure efficient and safe oil and gas production from shales.
2. Although recent efforts have allowed better assessment of the geochemical nature of gas shale systems, process understanding in time and space remains fragmentary concerning phase behavior prediction, during polyphasic geological history but also during production.
3. As interest in gas shales has recently been superseded by the search for and production of liquids in shales and associated strata, better documenting polarity and wettability of shale formations has de facto become a new challenge.
4. Future research should also be directed toward improved strategic accumulative risk assessment tools and methodologies that may ensure the minimization of the environmental impact of oil and gas production from shale and of potential hazards that might arise from shale gas activities.

DISCLOSURE STATEMENT

The authors are not aware of any affiliations, memberships, funding, or financial holdings that might be perceived as affecting the objectivity of this review.

ACKNOWLEDGMENTS

STXM data shown here were acquired at beamline 5.3.2.2 at the Advanced Light Source, which is supported by the Director of the Office of Science, US Department of Energy, under contract DEAC02-05CH11231, and at beamline 10ID-1 at the Canadian Light Source, which is supported by the Natural Sciences and Engineering Research Council of Canada, the Canadian Institutes of Health Research, the National Research Council Canada, and the University of Saskatchewan.

LITERATURE CITED

Ambrose RJ, Hartman RC, Diaz-Campos M, Akkutlu IY, Sondergeld CH. 2010. *New pore-scale considerations for shale gas in place calculations*. Presented at Soc. Pet. Eng. Unconv. Gas Conf., Feb. 23–25, Pittsburgh, PA. doi: 10.2118/131772-MS

Aplin AC, Matenaar IF, McCarty DK, ven der Pluijm BA. 2006. Influence of mechanical compaction and clay mineral diagenesis on the microfabric and pore-scale properties of deep-water Gulf of Mexico mudstones. *Clays Clay Miner.* 54:500–14

Armor JN. 2013. Emerging importance of shale gas to both the energy & chemicals landscape. *J. Energy Chem.* 22:21–26

Arthur MA, Sageman BB. 1994. Marine black shales: depositional mechanisms and environments of ancient deposits. *Annu. Rev. Earth Planet. Sci.* 22:499–551

Bai B, Elgmati M, Zhang H, Wei M. 2013. Rock characterization of Fayetteville shale gas plays. *Fuel* 105:645–52

Behar F, Lorant F, Mazeas L. 2008. Elaboration of a new compositional kinetic schema for oil cracking. *Org. Geochem.* 39:764–82

Behar F, Roy S, Jarvie D. 2010. Artificial maturation of a Type I kerogen in closed system: mass balance and kinetic modelling. *Org. Geochem.* 41:1235–47

Bera B, Sushanta MK, Douglas V. 2011. Understanding the micro structure of Berea Sandstone by the simultaneous use of micro-computed tomography (micro-CT) and focused ion beam-scanning electron microscopy (FIB-SEM). *Micron* 42:412–18

Bernard S, Benzerara K, Beyssac O, Brown GE Jr. 2010a. Multiscale characterization of pyritized plant tissues in blueschist facies metamorphic rocks. *Geochim. Cosmochim. Acta* 74:5054–68

Bernard S, Benzerara K, Beyssac O, Brown GE Jr, Stamm LG, Duringer P. 2009. Ultrastructural and chemical study of modern and fossil sporoderms by scanning transmission X-ray microscopy (STXM). *Rev. Palaeobot. Palynol.* 156:248–61

Bernard S, Bowen L, Wirth R, Schreiber A, Schulz HM, et al. 2013. FIB-SEM and TEM investigations of an organic-rich shale maturation series from the Lower Toarcian Posidonia Shale, Germany: nanoscale pore system and fluid-rock interactions. In *Electron Microscopy of Shale Hydrocarbon Reservoirs*, ed. W Camp, E Diaz, B Wawak, pp. 53–66. AAPG Mem. 102. Tulsa, OK: AAPG

Bernard S, Horsfield B, Schulz HM, Schreiber A, Wirth R, et al. 2010b. Multi-scale detection of organic and inorganic signatures provides insights into gas shale properties and evolution. *Chem. Erde Geochem.* 70(Suppl. 3):119–33

Bernard S, Horsfield B, Schulz HM, Wirth R, Schreiber A, Sherwood N. 2012a. Geochemical evolution of organic-rich shales with increasing maturity: a STXM and TEM study of the Posidonia Shale (Lower Toarcian, northern Germany). *Mar. Pet. Geol.* 31:70–89

Bernard S, Wirth R, Schreiber A, Schulz HM, Horsfield B. 2012b. Formation of nanoporous pyrobitumen residues during maturation of the Barnett Shale (Fort Worth Basin). *Int. J. Coal Geol.* 103:3–11

Bluhm H, Andersson K, Araki T, Benzerara K, Brown GE, et al. 2006. Soft X-ray microscopy and spectroscopy at the molecular environmental science beamline at the Advanced Light Source. *J. Electron Spectrosc. Relat. Phenom.* 150:86–104

Boyer C, Clark B, Jochen V, Lewis R, Miller CK. 2011. Shale gas: a global resource. *Oilfield Rev.* 23:28–39

Bustin AMM, Bustin RM, Cui X. 2008. *Importance of fabric on the production of gas shales*. Presented at Soc. Pet. Eng. Unconv. Reserv. Conf., Feb. 10–12, Keystone, CO. doi: 10.2118/114167-MS

Bustin AMM, Bustin RM. 2012. Importance of rock properties on the producibility of gas shales. *Int. J. Coal Geol.* 103:132–47

Chalmers GRL, Bustin RM, Power IM. 2012a. Characterization of gas shale pore systems by porosimetry, pycnometry, surface area and FE-SEM/TEM image analysis: examples from the Barnett, Woodford, Haynesville, Marcellus, and Doig formations. *AAPG Bull.* 96:1099–119

Chalmers GRL, Ross DJK, Bustin RM. 2012b. Geological controls on matrix permeability of Devonian Gas Shales in the Horn River and Liard basins, northeastern British Columbia, Canada. *Int. J. Coal Geol.* 103:120–31

Choquett PW, Pray LC. 1970. Geologic nomenclature and classification of porosity in sedimentary carbonates. *AAPG Bull.* 54:207–44

Clarkson CR, Freeman M, He L, Agamalian M, Melnichenko YB, et al. 2012. Characterization of tight gas reservoir pore structure using USANS/SANS and gas adsorption analysis. *Fuel* 95:371–85

Clarkson CR, Solano N, Bustin RM, Bustin AMM, Chalmers GRL, et al. 2013. Pore structure characterization of North American shale gas reservoirs using USANS/SANS, gas adsorption, and mercury intrusion. *Fuel* 103:606–16

Cooles GP, Mackenzie AS, Quigley TM. 1986. Calculation of petroleum masses generated and expelled from source rocks. *Org. Geochem.* 10:235–45

Curtis JB. 2002. Fractured shale-gas systems. *AAPG Bull.* 86:1921–38

Curtis ME, Ambrose RJ, Sondergeld CH, Rai CS. 2011a. *Investigation of the relationship between organic porosity and thermal maturity in the Marcellus Shale*. Presented at N. Am. Unconv. Gas Conf. Exhib., June 14–16, The Woodlands, TX. doi: 10.2118/144370-MS

Curtis ME, Ambrose RJ, Sondergeld CH, Rai CS. 2011b. *Transmission and scanning electron microscopy investigation of pore connectivity of gas shales on the nanoscale*. Presented at N. Am. Unconv. Gas Conf. Exhib., June 14–16, The Woodlands, TX. doi: 10.2118/144391-MS

Curtis ME, Ambrose RJ, Sondergeld CH, Rai CS. 2012a. Microstructural investigation of gas shales in two and three dimensions using nanometer-scale resolution imaging. *AAPG Bull.* 96:665–77

Curtis ME, Cardott BJ, Sondergeld CH, Rai CS. 2012b. Development of organic porosity in the Woodford Shale with increasing thermal maturity. *Int. J. Coal Geol.* 103:26–31

Curtis ME, Cardott BJ, Sondergeld CH, Rai CS. 2012c. *The development of organic porosity in the Woodford Shale as a function of thermal maturity*. Presented at Soc. Pet. Eng. Ann. Tech. Conf. Exhib., Oct. 8–10, San Antonio, TX. doi: 10.2118/160158-MS

Curtis ME, Sondergeld CH, Ambrose RJ, Rai CS. 2010. *Structural characterization of gas shales on the micro- and nano-scales*. Presented at Can. Unconv. Resour. Int. Pet. Conf., Oct. 19–21, Calgary. doi: 10.2118/137693-MS

Dacy JM. 2010. *Core tests for relative permeability of unconventional gas reservoirs.* Presented at Soc. Pet. Eng. Ann. Tech. Conf. Exhib., Sept. 19–22, Florence, Italy. doi: 10.2118/135427-MS

Dembicki HJ. 2009. Three common source rock evaluation errors made by geologists during prospect or play appraisals. *AAPG Bull.* 93:341–56

Desbois G, Urai JL, Erez-Willard FP, Radi Z, Offern S, et al. 2013. Argon broad ion beam tomography in a cryogenic scanning electron microscope: a novel tool for the investigation of representative microstructures in sedimentary rocks containing pore fluid. *J. Microsc.* 249:215–35

Desbois G, Urai JL, Houben ME, Sholokhova Y. 2010. Typology, morphology and connectivity of pore space in claystones from reference site for research using BIB, FIB and cryo-SEM methods. *EPJ Web Conf.* 6:22005. doi: 10.1051/epjconf/20100622005

di Primio R. 2002. Unraveling secondary migration effects through the regional evaluation of PVT data: a case study from Quadrant 25, NOCS. *Org. Geochem.* 33:643–53

di Primio R, Dieckmann N, Mills N. 1998. PVT and phase behaviour analysis in petroleum exploration. *Org. Geochem.* 29:207–22
Dieckmann V, Ondrak R, Cramer B, Horsfield B. 2006. Deep basin gas: new insights from kinetic modelling and isotopic fractionation in deep-formed gas precursors. *Mar. Pet. Geol.* 23:183–99
Dieckmann V, Schenk HJ, Horsfield B, Welte DH. 1998. Kinetics of petroleum generation and cracking by programmed-temperature closed-system pyrolysis of Toarcian Shales. *Fuel* 77:23–31
Driskill B, Walls J, Sinclair SW, DeVito J. 2013. Applications of SEM imaging to reservoir characterization in the Eagle Ford Shale, south Texas, U.S.A. In *Electron Microscopy of Shale Hydrocarbon Reservoirs*, ed. W Camp, E Diaz, B Wawak, pp. 115–36. AAPG Mem. 102. Tulsa, OK: AAPG
Ehrenberg SN, Walderhaug O, Bjorlykke K. 2012. Carbonate porosity creation by mesogenetic dissolution: reality or illusion? *AAPG Bull.* 96:217–33
Elgmati M, Zhang H, Bai B, Flori R. 2011a. *Submicron-pore characterization of shale gas plays*. Presented at N. Am. Unconv. Gas Conf. Exhib., June 14–16, The Woodlands, TX. doi: 10.2118/144050-MS
Elgmati M, Zobaa M, Zhang H, Bai B, Oboh-Ikuenobe F. 2011b. *Palynofacies analysis and submicron pore modeling of shale-gas plays*. Presented at N. Am. Unconv. Gas Conf. Exhib., June 14–16, The Woodlands, TX. doi: 10.2118/144267-MS
Emmanuel S, Day-Stirrat RJ. 2012. A framework for quantifying size dependent deformation of nano-scale pores in mudrocks. *J. Appl. Geophys.* 86:29–35
Erdmann M, Horsfield B. 2006. Enhanced late gas generation potential of petroleum source rocks via recombination reactions: evidence from the Norwegian North Sea. *Geochim. Cosmochim. Acta* 70:3943–56
Guo GL, Xianming X, Hui T, Zhiguang S. 2009. Distinguishing gases derived from oil cracking and kerogen maturation: insights from laboratory pyrolysis experiments. *Org. Geochem.* 40:1074–84
Hao F, Zou H. 2013. Cause of shale gas geochemical anomalies and mechanisms for gas enrichment and depletion in high-maturity shales. *Mar. Pet. Geol.* 44:1–12
Heath JE, Dewers TA, McPherson BJOL, Petrusak R, Chidsey TC, et al. 2011. Pore networks in continental and marine mudstones: characteristics and controls on sealing behavior. *Geosphere* 7:429–54
Hill RJ, Tang YC, Kaplan IR. 2003. Insights into oil cracking based on laboratory experiments. *Org. Geochem.* 34:1651–72
Horsfield B. 1989. Practical criteria for classifying kerogens: some observations from pyrolysis–gas chromatography. *Geochim. Cosmochim. Acta* 53:891–901
Horsfield B, Dueppenbecker SJ. 1991. The decomposition of Posidonia Shale and Green River shale kerogens using microscale sealed vessel (MSSV) pyrolysis. *J. Anal. Appl. Pyrolysis* 20:107–23
Horsfield B, Schenk H, Mills N, Welte D. 1992. An investigation of the in-reservoir conversion of oil to gas: compositional and kinetic findings from closed-system programmed-temperature pyrolysis. *Org. Geochem.* 19:191–204
Jarvie DM, Hill RJ, Ruble TE, Pollastro RM. 2007. Unconventional shale-gas systems: the Mississippian Barnett Shale of north-central Texas as one model for thermogenic shale-gas assessment. *AAPG Bull.* 91:475–99
Javadpour F. 2009. Nanopores and apparent permeability of gas flow in mudrocks (shales and siltstone). *J. Can. Pet. Technol.* 48:16–21
Javadpour F, Fiser D, Unsworth M. 2007. Nanoscale gas flow in shale gas sediments. *J. Can. Pet. Technol.* 46:55–61
Javadpour F, Farshi MM, Amrein M. 2012. Atomic-force microscopy: a new tool for gas-shale characterization. *J. Can. Pet. Technol.* 51:236–43
Jenkins C, Boyer C. 2008. Coalbed and shale-gas reservoirs. *J. Pet. Technol.* 60:92–99
Josh M, Esteban L, Delle Piane C, Sarout J, Dewhurst DN, Clennell MB. 2012. Laboratory characterisation of shale properties. *J. Pet. Sci. Eng.* 88–89:107–24
Katsube TJ, Williamson MA. 1994. Effects of diagenesis on shale nano-pore structure and implications for sealing capacity. *Clay Miner.* 29:451–61
Kaznatcheev KV, Karunakaran C, Lanke UD, Urquhart SG, Obst M, Hitchcock AP. 2007. Soft X-ray spectromicroscopy beamline at the CLS: commissioning results. *Nucl. Instrum. Methods Phys. Res. A* 582:96–99
Kelemen SR, Afeworki M, Gorbaty ML, Sansone M, Kwiatek PJ, et al. 2007. Direct characterization of kerogen by X-ray and solid-state ^{13}C nuclear magnetic resonance methods. *Energy Fuels* 21:1548–61

Kilcoyne ALD, Tyliszczak T, Steele WF, Fakra S, Hitchcock P, et al. 2003. Interferometer-controlled scanning transmission X-ray microscopes at the Advanced Light Source. *J. Synchrotron Radiat.* 10:125–36

Kim JW, Bryant WR, Watkins JS, Tieh TT. 1999. Electron microscopic observations of shale diagenesis, offshore Louisiana, USA, Gulf of Mexico. *Geo-Marine Lett.* 18:234–40

Klaver J, Desbois G, Urai JL, Littke R. 2012. BIB-SEM study of the pore space morphology in early mature Posidonia Shale from the Hils area, Germany. *Int. J. Coal Geol.* 103:12–25

Krooss BM, van Bergen F, Gensterblum Y, Siemons N, Pagnier HJM, David P. 2002. High-pressure methane and carbon dioxide adsorption on dry and moisture-equilibrated Pennsylvanian coals. *Int. J. Coal Geol.* 51:69–92

Kuhn PP, di Primio R, Hill R, Lawrence JR, Horsfield B. 2012. Three-dimensional modeling study of the low-permeability petroleum system of the Bakken Formation. *AAPG Bull.* 96:1867–97

Kwon O, Kronenberg AK, Gangi AF, Johnson B, Herbert BE. 2004. Permeability of illite-bearing shale. 1. Anisotropy and effects of clay content and loading. *J. Geophys. Res.* 109:B10205

Lewan MD, Roy S. 2011. Role of water in hydrocarbon generation from Type-I kerogen in Mahogany oil shale of the Green River Formation. *Org. Geochem.* 42:31–41

Lewan MD, Winters JC, McDonald JH. 1979. Generation of oil-like pyrolyzates from organic-rich shales. *Science* 203:897–99

Lis GP, Mastalerz M, Schimmelmann A, Lewan MD, Stankiewicz BA. 2005. FTIR absorption indices for thermal maturity in comparison with vitrinite reflectance R_0 in type-II kerogens from Devonian black shales. *Org. Geochem.* 36:1533–52

Littke R, Krooss B, Uffmann AK, Schulz HM, Horsfield B. 2011. Unconventional gas resources in the Paleozoic of Central Europe. *Oil Gas Sci. Technol.* 66:953–77

Lorant F, Behar F. 2002. Late generation of methane from mature kerogens. *Energy Fuels* 16:412–27

Loucks RG, Reed RM, Ruppel SC, Hammes U. 2010. Preliminary classification of matrix pores in mudrocks. *Gulf Coast Assoc. Geol. Soc. Trans.* 60:435–41

Loucks RG, Reed RM, Ruppel SC, Hammes U. 2012. Spectrum of pore types and networks in mudrocks and a descriptive classification for matrix-related mudrock pores. *AAPG Bull.* 96:1071–98

Loucks RG, Reed RM, Ruppel SC, Jarvie DM. 2009. Morphology, genesis, and distribution of nanometer-scale pores in siliceous mudstones of the Mississippian Barnett Shale. *J. Sediment. Res.* 79:848–61

Mahlstedt N, Horsfield B. 2012. Metagenetic methane generation in gas shales. I. Screening protocols using immature samples. *Mar. Pet. Geol.* 31:27–42

Mahlstedt N, Horsfield B, Dieckmann V. 2008. Second order reactions as a prelude to gas generation at high maturity. *Org. Geochem.* 39:1125–29

Mao J, Fang X, Lan Y, Schimmelmann A, Mastalerz M, et al. 2010. Chemical and nanometer-scale structure of kerogen and its change during thermal maturation investigated by advanced solid-state ^{13}C NMR spectroscopy. *Geochim. Cosmochim. Acta* 74:2110–27

Mazzullo SJ, Harris PM. 1992. Mesogenetic dissolution: its role in porosity development in carbonate reservoirs. *AAPG Bull.* 76:607–20

McGlade C, Speirs J, Sorrell S. 2013. Unconventional gas—a review of regional and global resource estimates. *Energy* 55:571–84

Mehmani A, Tokan-Lawal A, Prodanović M, Sheppard AP. 2011. *The effect of microporosity on transport properties in tight reservoirs*. Presented at N. Am. Unconv. Gas Conf. Exhib., June 14–16, The Woodlands, TX. doi: 10.2118/144384-MS

Milliken KL, Esch WL, Reed RM, Zhang TW. 2012. Grain assemblages and strong diagenetic overprinting in siliceous mudrocks, Barnett Shale (Mississippian), Fort Worth Basin, Texas. *AAPG Bull.* 96:1553–78

Milliken KL, Reed RM. 2010. Multiple causes of diagenetic fabric anisotropy in weakly consolidated mud, Nankai Accretionary Prism, IODP Expedition 316. *J. Struct. Geol.* 32:1887–98

Mondol NH, Bjorlykke K, Jahren J. 2008. Experimental compaction of clays: relationship between permeability and petrophysical properties in mudstones. *Pet. Geosci.* 14:319–37

Montgomery SL, Jarvie DM, Bowker KA, Pollastro RM. 2005. Mississippian Barnett Shale, Fort Worth Basin, north-central Texas: gas-shale play with multi-trillion cubic foot potential. *AAPG Bull.* 89:155–75

Muscio GPA, Horsfield B, Welte DH. 1994. Occurrence of thermogenic gas in the immature zone—implications from the Bakken in-source reservoir system. *Org. Geochem.* 22:461–76

Nelson PH. 2009. Pore throat sizes in sandstones, tight sandstones, and shales. *AAPG Bull.* 93:1–13
Orr C. 1977. Pore size and volume measurement. In *Treatise on Analytical Chemistry, Part III: Analytical Chemistry in Industry*, ed. IM Kolthoff, PJ Elving, FH Stross, pp. 321–58. New York: Wiley
Pan C, Jiang L, Liu J, Zhang S, Zhu G. 2012. The effects of pyrobitumen on oil cracking in confined pyrolysis experiments. *Org. Geochem.* 45:29–47
Passey QR, Bohacs KM, Esch WL, Klimentidis R, Sinha S. 2010 . *From oil-prone source rock to gas-producing shale reservoir—geologic and petrophysical characterization of unconventional shale gas reservoirs.* Presented at Int. Oil Gas Conf. Exhib. China, June 8–10, Beijing. doi: 10.2118/131350-MS
Pepper AS, Corvi PJ. 1995. Simple kinetic models of petroleum formation. Part I: oil and gas generation from kerogen. *Mar. Pet. Geol.* 12:291–319
Pepper AS, Dodd TA. 1995. Simple kinetic models of petroleum formation. Part II: oil-gas cracking. *Mar. Pet. Geol.* 12:321–40
Petersen HI, Rosenberg P, Nytoft HP. 2008. Oxygen groups in coals and alginite-rich kerogen revisited. *Int. J. Coal Geol.* 74:93–113
Pittman ED. 1979. Porosity, diagenesis and productive capability of sandstone reservoirs. In *Aspects of Diagenesis*, ed. PA Scholle, PR Schluger, pp. 159–73. SEPM Spec. Publ. 26. Tulsa, OK: SEPM
Rodriguez ND, Philp RP. 2010. Geochemical characterization of gases from the Mississippian Barnett Shale, Fort Worth Basin, Texas. *AAPG Bull.* 94:1641–56
Ross DJ, Bustin RM. 2009. The importance of shale composition and pore structure upon gas storage potential of shale gas reservoirs. *Mar. Pet. Geol.* 26:916–27
Ruppert L, Sakurovs R, Blach TP, He L, Melnichenko YB, et al. 2013. A USANS/SANS study of the accessibility of pores in the Barnett shale to methane and water. *Energy Fuels* 27:772–79
Santamaria-Orozco D, Horsfield B. 2003. Gas generation potential of Upper Jurassic (Tithonian) source rocks in the Sonda de Campeche, Mexico. In *The Circum-Gulf of Mexico and the Caribbean: Hydrocarbon Habitats, Basin Formation, and Plate Tectonics*, ed. C Bartolini, RT Buffler, J Blickwede, pp. 349–63. AAPG Mem. 79. Tulsa, OK: AAPG
Schenk HJ, di Primio R, Horsfield B. 1997. The conversion of oil into gas in petroleum reservoirs. Part 1: comparative kinetic investigation of gas generation from crude oils of lacustrine, marine and fluviodeltaic origin by programmed-temperature closed-system pyrolysis. *Org. Geochem.* 26:467–81
Schenk HJ, Dieckmann V. 2004. Prediction of petroleum formation: the influence of laboratory heating rates on kinetic parameters and geological extrapolations. *Mar. Pet. Geol.* 21:79–95
Schenk HJ, Horsfield B. 1998. Using natural maturation series to evaluate the utility of parallel reaction kinetics models: an investigation of Toarcian shales and Carboniferous coals, Germany. *Org. Geochem.* 29:154–99
Schieber J. 2010. *Common themes in the formation and preservation of porosity in shales and mudstones—illustrated with examples across the Phanerozoic.* Presented at Soc. Pet. Eng. Unconv. Gas Conf., Feb. 23–25, Pittsburgh, PA. doi: 10.2118/132370-MS
Schneider J, Flemings PB, Day-Stirrat RJ, Germaine JT. 2011. Insights into pore-scale controls on mudstone permeability through resedimentation experiments. *Geology* 39:1011–14
Seewald JS, Benitez-Nelson BC, Whelan JK. 1998. Laboratory and theoretical constraints on the generation and composition of natural gas. *Geochim. Cosmochim. Acta* 62:1599–617
Slatt RM, O'Brien NR. 2011. Pore types in the Barnett and Woodford gas shales: contribution to understanding gas storage and migration pathways in fine-grained rocks. *AAPG Bull.* 95:2017–30
Slatt RM, Rodriguez ND. 2012. Comparative sequence stratigraphy and organic geochemistry of gas shales: commonality or coincidence? *J. Nat. Gas Sci. Eng.* 8:68–84
Smernik RJ, Schwark L, Schmidt MWI. 2006. Assessing the quantitative reliability of solid-state ^{13}C NMR spectra of kerogens across a gradient of thermal maturity. *Solid State Nucl. Magn. Reson.* 29:312–21
Snowdon LR. 1979. Errors in extrapolation of experimental kinetic parameters to organic geochemical systems. *AAPG Bull.* 63:1128–38
Sondergeld CH, Ambrose RJ, Rai CS, Moncrieff J. 2010. *Micro-structural studies of gas shales*. Presented at Soc. Pet. Eng. Unconv. Gas Conf., Feb. 23–25, Pittsburgh, PA. doi: 10.2118/131771-MS
Sorby HC. 1908. On the application of quantitative methods to the study of the structure and history of rocks. *Q. J. Geol. Soc.* 64:171–232

Stasiuk LD. 1997. The origin of pyrobitumens in Upper Devonian Leduc Formation gas reservoirs, Alberta, Canada: an optical and EDS study of oil to gas transformation. *Mar. Pet. Geol.* 14:915–29

Strapoc D, Mastalerz M, Schimmelmann A, Drobniak A, Hasenmueller NR. 2010. Geochemical constraints on the origin and volume of gas in the New Albany Shale (Devonian–Mississippian), eastern Illinois Basin. *AAPG Bull.* 94:1713–40

Tian H, Xiao X, Wilkins RWT, Tang Y. 2008. New insights into the volume and pressure changes during the thermal cracking of oil to gas in reservoirs: implications for the in-situ accumulation of gas cracked from oils. *AAPG Bull.* 92:181–200

Tiem VTA, Horsfield B, Sykes R. 2008. Influence of in-situ bitumen on the generation of gas and oil in New Zealand coals. *Org. Geochem.* 39:1606–19

Tilley B, McLellan S, Hiebert S, Quartero B, Veilleux B, Muehlenbachs K. 2011. Gas isotope reversals in fractured gas reservoirs of the western Canadian Foothills: mature shale gases in disguise. *AAPG Bull.* 95:1399–422

US Energy Inf. Adm. (EIA). 2013. *Annual Energy Outlook 2013*. Washington, DC: US EIA. **http://www.eia.gov/forecasts/aeo/pdf/0383(2013).pdf**

Walls JD, Sinclair SW. 2011. Eagle Ford shale reservoir properties from digital rock physics. *First Break* 29:97–101

Wang FP, Reed RM. 2009. *Pore networks and fluid flow in gas shales*. Presented at Soc. Pet. Eng. Ann. Tech. Conf. Exhib., Oct. 4–7, New Orleans, LA. doi: 10.2118/124253-MS

Wei ZB, Gao XX, Zhang DJ, Da J. 2005. Assessment of thermal evolution of kerogen geopolymers with their structural parameters measured by solid-state ^{13}C NMR spectroscopy. *Energy Fuels* 19:240–50

Weijermars R. 2013. Economic appraisal of shale gas plays in Continental Europe. *Appl. Energy* 106:100–15

Xingang Z, Jiaoli K, Bei L. 2013. Focus on the development of shale gas in China based on SWOT analysis. *Renew. Sustain. Energy Rev.* 21:603–13

Yang Y, Aplin AC. 2010. A permeability-porosity relationship for mudstones. *Mar. Pet. Geol.* 27:1692–97

Zumberge J, Ferworn K, Brown S. 2012. Isotopic reversal ("rollover") in shale gases produced from the Mississippian Barnett and Fayetteville formations. *Mar. Pet. Geol.* 31:43–52